

# Friction Coefficients and Directed Motion of Asymmetric Test Particles

K. Handrich<sup>1</sup> and F.-P. Ludwig<sup>1</sup>

*Received September 28, 1995; final August 12, 1996*

---

The behavior of a test particle in a rarefied gas of classical particles is investigated, considering different interaction mechanisms (specular and diffuse reflection, respectively). For large mass ratio between test and gas particles, analytical expressions for the linear friction coefficient are derived. Moreover, the existence of directed motion of asymmetric test particles with distinct initial conditions (but in the absence of any gradients) is shown. The analytical results are supported by a numerical simulation technique applicable to systems with any mass ratio, which is described here in detail.

---

**KEY WORDS:** Brownian motion; friction coefficients; fluctuation-induced transport; numerical simulation.

## 1. INTRODUCTION

Since Einstein's work in 1905<sup>(1)</sup> the physical problem of Brownian motion has been the subject of numerous investigations, both theoretical and experimental. With the development of computers, numerical methods have become increasingly important.<sup>(2-5)</sup> Brownian particles have a very large mass compared with the particles of the surrounding medium. This fact plays an important role in the analytical treatment.<sup>(6)</sup> By means of computer simulations, it is possible to investigate in detail Brownian particles (or test particles) with masses comparable with the medium particles.<sup>(7-11)</sup> In most cases one is interested in the behavior of the velocity autocorrelation function of the test particles characteristic for different properties of the system under consideration.<sup>(7)</sup>

---

<sup>1</sup> Institut für Physik, Technische Universität Ilmenau, D-98693 Ilmenau, Germany.

In recent years, inspired by the study of biological systems in which some kind of directed thermal motion may occur, the problem of Brownian motion has again attracted the interest of physicists (for a review, see ref. 12 and the papers cited therein). It has been shown both experimentally and theoretically that under certain (nonequilibrium) conditions directed transport of particles can be extracted from the white noise of a thermal bath.

In this paper we present analytical and numerical results for a classical model suggested in ref. 13. In the interaction of our test particles with the gas particles we distinguish the usual specular reflection and completely diffuse elastic reflection.

The numerical simulation technique is described in detail. In the analytical part we derive expressions for the linear friction coefficients of specular reflecting, diffuse reflecting, and asymmetric test particles, respectively, for the case of a large mass ratio  $M/m \gg 1$  ( $M$  is the mass of the test particle,  $m$  is the mass of the gas particle). Moreover, we show the existence of directed acceleration of a test particle as long as it is not completely in equilibrium with its environment.

Then the analytical results are confirmed and illustrated by a numerical simulation.

## 2. MODEL

For simplification of the numerical and analytical treatment, we choose flat planar test particles (TP) with their surface normals fixed parallel to the  $x$  axis of the laboratory system<sup>(13, 14)</sup> (see Fig. 1). The length of the edges (or diameter) of the TP is large in comparison with its thickness; thus the contribution of the edges to the motion of the TP can be neglected. Moreover, the rotational degrees of freedom of the test particle are not considered here.

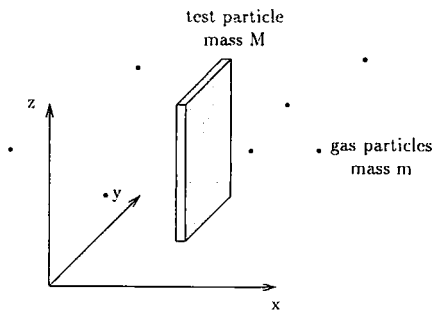


Fig. 1. Model of the planar test particle.

As a physical example one could imagine test particles with spontaneous magnetization in the direction perpendicular to their planes, located in a sufficiently strong external magnetic field.

The motion of the TP results from collisions with the surrounding gas particles (GP), which are treated as classical particles. The medium gas is assumed to be in thermodynamic equilibrium at every moment. Additionally, it is sufficiently rarefied that "snowplough effects" and recollisions of the test particles do not play a role, i.e., the gas particles in the environment of the test particle always have a Maxwell velocity distribution.<sup>(15)</sup>

First we need the flux of gas particles to the planes of the TP. In the following we always refer to the left-hand side of the TP, if not mentioned otherwise. The TP is moving in the laboratory system with the velocity  $\mathbf{u} = (u_x, u_y, u_z)$ . The flux of GP to the left-hand face of the TP, i.e., the number of incident particles per time, is

$$\frac{dN}{dt} = nA \int_{v_x \geq u_x} (v_x - u_x) f_M(\mathbf{v}) d\mathbf{v} \quad (1)$$

$n$  is the number density of the medium gas,  $A$  the surface area of the TP, and  $\mathbf{v}$  the velocity of the gas particles. The distribution function of the GP velocities is a Maxwell distribution

$$f_M(\mathbf{v}) d^3v = \left(\frac{m}{2\pi kT}\right)^{3/2} \exp\left(-\frac{m\mathbf{v}^2}{2kT}\right) d^3v \quad (2)$$

with the mass  $m$  of the GP and the temperature  $T$  of the gas.

For simplification, we introduce reduced velocities  $\mathbf{v}^*$ ,  $\mathbf{u}^*$  and a reduced time scale  $t^*$ :

$$\mathbf{v} = \sqrt{\frac{kT}{m}} \mathbf{v}^*, \quad \mathbf{u} = \sqrt{\frac{kT}{m}} \mathbf{u}^*, \quad t = \frac{1}{nA} \sqrt{\frac{2\pi m}{kT}} t^* \quad (3)$$

Then (1) with (2) reads

$$\frac{dN}{dt^*} = \frac{1}{2\pi} \int_{v_x^* \geq u_x^*} (v_x^* - u_x^*) \exp\left(-\frac{1}{2} v^{*2}\right) d^3v^* \quad (4)$$

In the following we omit the asterisk and always refer to the reduced variables. Now we perform the integration in (4) over the velocities  $u_x \leq v_x \leq +\infty$  and  $-\infty \leq v_{y,z} \leq +\infty$  of the GP and get the total flux  $J_l$

to the left-hand surface of the TP. With the notation  $\tau_l$  for the mean time between two impacts on the left-hand side of the TP, we get

$$\frac{dN}{dt} = J_l(u_x) = \frac{1}{\tau_l} = \exp\left(-\frac{1}{2}u_x^2\right) + u_x \sqrt{\frac{\pi}{2}} \left[ \operatorname{erf}\left(\frac{u_x}{\sqrt{2}}\right) - 1 \right] \quad (5)$$

with the definition of the error function

$$\operatorname{erf}(x) := \frac{2}{\sqrt{\pi}} \int_0^x e^{-\xi^2} d\xi$$

In order to get the flux to the right-hand side of the TP, we simply replace  $u_x$  by  $-u_x$  in (5).

For large masses of the TP,  $u_x \approx 0$  holds, and the mean time between two impacts on the TP becomes independent of  $u_x$ . Taking into account both sides of the particle, we find for the mean time between two collisions of a TP at rest (in nonreduced units)

$$\tau_0 = \frac{1}{2nA} \sqrt{\frac{2\pi m}{kT}} = \frac{2}{nA \langle v \rangle} \quad (6)$$

with  $\langle v \rangle$  the mean magnitude of the GP velocities.

At constant  $u_x$  the flux of incident GP is not dependent on time. Therefore, in the numerical simulation one can treat the impact times and the velocities of the incident particles as independent of each other. First we look for the distribution function of the time intervals between two successive impacts of GP on the faces of the TP. Let  $t=0$  be the moment of the last foregoing collision between the TP and a GP. In order to derive the distribution function of interest, we divide the time interval  $[0 \cdots t]$  into  $\nu$  subintervals which all have the same size  $\Delta t$ .<sup>(14)</sup> Let  $\nu$  be sufficiently large for the subintervals to be very small. In the sense of a Markov process, the events in all subintervals are assumed to be statistically completely independent. The probability of an impact of a gas particle on the left-hand side of the test particle is the same in each of the subintervals. As long as  $u_x = \text{const}$ , the GP hit the left-hand side of the TP with a constant frequency  $1/\tau_l$  and

$$\Delta p = \frac{\Delta t}{\tau_l}$$

is the probability of a collision in  $\Delta t$ .

Now we assume the TP to be hit by a GP exactly in the  $(\nu + 1)$ th sub-interval without preceding hits in the interval  $[0 \dots t]$ . The probability for that event is

$$\Delta P = \left(1 - \frac{\Delta t}{\tau_l}\right)^\nu \frac{\Delta t}{\tau_l} \quad (7)$$

We substitute  $\nu$  by  $t/\Delta t$  and rewrite (7):

$$\Delta P = \left(1 - \frac{\Delta t}{\tau_l}\right)^{t/\Delta t} \frac{\Delta t}{\tau_l} = \left[\left(1 - \frac{\Delta t}{\tau_l}\right)^{-\tau_l/\Delta t}\right]^{-t/\tau_l} \frac{\Delta t}{\tau_l} \quad (8)$$

In the limit  $\Delta t \rightarrow 0$  it follows from

$$\lim_{\varepsilon \rightarrow 0} (1 - \varepsilon)^{-1/\varepsilon} = e$$

that

$$dP = F(t) dt = \frac{1}{\tau_l} \exp\left(-\frac{t}{\tau_l}\right) dt \quad (9)$$

$F(t)$  is the distribution function of the time intervals between two successive impacts of GP on the left-hand side of the TP if the average flux to the left-hand TP face is  $1/\tau_l$ . For the distribution function on the right-hand side, one simply substitutes  $u_x$  by  $-u_x$  in (5) and inserts the resulting  $\tau_r$  into (9). The assumption of a Markov process in the derivation of (9) implicitly supposes that memory effects of the medium gas can be neglected. In particular, short-time recollisions between GP and TP are excluded. This assumption is reasonable for very heavy TP, where the GP are moving with much higher velocities and escaping very fast from the TP after a collision.

However, even in the case of small mass ratios  $M \approx m$ , the assumption of a Markov velocity process is permitted within our three-dimensional model system. The medium particles are moving with a mean velocity  $\langle v_l \rangle$  in the tangential direction relative to the test particle.  $\tau$  is the mean free time of the TP, and  $d$  its diameter (or length of the edges). If the condition

$$d \ll \langle v_l \rangle \tau$$

is fulfilled, the GP cross the spatial region passed by the TP in a very short time compared to the mean free time of the TP. The possibility of a recollision between the TP and a particular GP can be made arbitrary small by

increasing the mean free time  $\tau$ . Thus, assuming a very rarefied medium gas, the conditions of a Markov process are fulfilled.

Now we are able to simulate the motion of our test particle due to the collisions with the surrounding gas particles in a very efficient way. The simulation runs as follows<sup>(14)</sup>:

1. The mean collision frequencies corresponding to the actual velocity  $u_x$  are calculated by (5) for the left-hand side and the right-hand side of the TP, respectively. According to the ratio of the incident fluxes to both faces of the TP, the side of the next impact of a GP is drawn. After that, the moment of the collision is drawn using (9) with the appropriate time constant  $\tau_{i,r}$ . Now the moment and the side of the next collision with a GP are defined.

2. The velocity of the incident GP is drawn. The probability density of the tangential velocity components  $v_x$  and  $v_z$  is given by the Maxwell distribution:

$$f_M(v_i) \sim \exp(-v_i^2/2), \quad i = y, z$$

The probability density of the normal velocity components follows from the incident flux of the gas particles:

$$\begin{aligned} f_j(v_x) &\sim (v_x - u_x) \exp(-v_x^2/2) & v_x > u_x & \text{(left-hand side)} \\ f_j(v_x) &\sim (u_x - v_x) \exp(-v_x^2/2) & v_x < u_x & \text{(right-hand side)} \end{aligned}$$

3. The velocity of the TP after the collision is calculated due to the special interaction mechanism (specular or diffuse reflection). Then the cycle starts again with the new velocity of the test particle.

Between the collisions the velocity of the TP is constant. The quantities of interest, such as the velocity distribution or the mean velocity of the TP, are saved for later analysis.

### 3. DIFFUSE-ELASTIC REFLECTION

A collision between TP and GP is called diffuse-elastic if it fulfills the following conditions:

1. The reflection is diffuse, i.e., GP hitting on the TP with a fixed incident angle are scattered into different directions. The distribution of the possible directions depends on the particular model considered.

2. The collision is completely elastic, i.e., the total kinetic energy of the colliding particles is conserved.

The problem of two interacting particles is commonly simplified by introduction of the center-of-mass velocity and the relative velocity of the particles. From the conservation laws of energy and momentum it follows that the magnitude of the relative velocity  $\mathbf{g} = \mathbf{v} - \mathbf{u}$  is conserved during a completely elastic collision. The diffuse reflection is simply a rotation of the vector of the relative velocity. Now we change into a coordinate system fixed at the TP. In this system the TP is at rest, and the GP hit the TP with the relative velocity  $\mathbf{g}$  and leave with the velocity  $\mathbf{g}'$ . We define the incident and reflection angles inside this system. Let  $\varphi$  be the angle between the projection of  $\mathbf{g}$  into the  $(y, z)$  plane and the  $y$  axis and  $\vartheta$  the polar angle between the velocity vector and the  $x$  axis, i.e., the surface normal of the TP face. Without violation of the conservation laws of energy and momentum any reflection angles  $\varphi'$  and  $\vartheta'$  may be chosen. The relative velocity of the particles after the collision is then

$$\begin{aligned} g'_x &= g \cos \vartheta' \\ g'_y &= g \sin \vartheta' \cos \varphi' \\ g'_z &= g \sin \vartheta' \sin \varphi' \end{aligned} \quad (10)$$

The simulation of the diffuse-elastic collision is restricted to the choice of the reflection angles  $\varphi'$  and  $\vartheta'$ . For simplification we assume all azimuth angles  $\varphi'$  to be equivalent and independent of the incident direction; thus  $\varphi'$  is uniformly distributed between 0 and  $2\pi$ .

It remains to find the distribution function of the polar angle  $\vartheta'$ . In the following the terms incident and reflection angles always refer to the polar angles  $\vartheta$  and  $\vartheta'$ .

### 3.1. Distribution Functions of Reflection Angles

In the simple case of specular reflection of the GP at the surface of the TP the reflection law  $\vartheta' = \vartheta$  holds. According to Lambert's law, completely diffuse reflection is described by a cosine-type distribution of the number of reflected particles depending on the reflection angle<sup>(16)</sup> ( $N$  vs.  $\vartheta'$ ). The distribution over the solid angle is  $dN \sim \cos \vartheta \sin \vartheta d\vartheta d\varphi$ , and with normalization the distribution function of the reflection angles is

$$2 \cos \vartheta' \sin \vartheta' d\vartheta' \quad (11)$$

## 4. RESULTS

### 4.1. Analytical Friction Coefficients

The motion of very heavy test particles in an environment of much lighter medium particles (Brownian motion) is commonly described by means of the Langevin equation<sup>(6)</sup>

$$\frac{du_x}{dt} = -\gamma u_x + a(t) \quad (12)$$

$\gamma u_x$  is the systematic friction force (strictly speaking, the friction acceleration) exerted on the test particle, averaged over a large number of collisions with the medium particles, and  $a(t)$  is the fluctuating random force. The formal solution of (12) is

$$u_x(t) = u_x(0) e^{-\gamma t} + e^{-\gamma t} \int_0^t e^{\gamma \xi} a(\xi) d\xi \quad (13)$$

Without random force, any initial velocity  $u_x(0)$  decays exponentially with time. The coefficient  $\gamma$  is called the linear friction coefficient of the test particle. Now we want to derive an expression for the friction coefficient of a TP with diffuse-elastic interaction and compare it with the friction coefficient of a specular reflecting particle. Moreover, the equation of motion of an asymmetric TP with one specular reflecting face and one diffuse reflecting face is investigated. We use again the TP-fixed coordinate system, where the GP are moving with the relative velocities  $\mathbf{g}$ . By integration of the velocity changes per single collision over the total flux of incident GP, one finds the average acceleration exerted on the TP as the result of the numerous collisions with the GP:

$$\begin{aligned} \frac{du_x}{dt} = & \int \int_{g_x > 0} \Delta u_x^{(l)}(\mathbf{g}) \cdot g_x f(\mathbf{g}, \mathbf{u}) d^3g \\ & - \int \int_{g_x < 0} \Delta u_x^{(r)}(\mathbf{g}) \cdot g_x f(\mathbf{g}, \mathbf{u}) d^3g \end{aligned} \quad (14)$$

The index  $l$  denotes the left-hand side of the TP, the index  $r$  the right-hand side (see Fig. 1).

The velocity change of the TP by a single collision is

$$\Delta u_x = u'_x - u_x = \frac{m}{M+m} (g_x - g'_x) = \pm \frac{m}{M+m} g (\cos \vartheta + \cos \vartheta') \quad (15)$$



The positive and negative signs hold on the left-hand side or on the right-hand side of the TP, respectively.

On specular reflection, in (15)  $\cos \vartheta' = \cos \vartheta$  holds. On completely diffuse reflection,  $\cos \vartheta'$  in (15) is replaced by its mean value due to the distribution function (11)

$$\langle \cos \vartheta' \rangle = 2 \int_0^1 \cos^2 \vartheta' d(\cos \vartheta') = \frac{2}{3} \quad (16)$$

because many single collisions contribute to the friction force.

In the TP-fixed coordinate system the entire gas medium is moving with the mean velocity  $-\mathbf{u}$ . The distribution function of the relative velocities in this system is

$$f(\mathbf{g}, \mathbf{u}) d^3g = \frac{1}{2\pi} \exp\left[-\frac{1}{2}(\mathbf{g} + \mathbf{u})^2\right] d^3g \quad (17)$$

Note that (17) is not normalized in the usual form, since the factor  $1/\sqrt{2\pi}$  is already contained in the reduced time scale [cf. (14), (3)].

Since the TP are much heavier than the gas particles,  $u \ll g$  holds for the magnitudes of the particle velocities. We expand (17) in a power series to first-order terms in  $\mathbf{u}$ :

$$\begin{aligned} f(\mathbf{g}, \mathbf{u}) d^3g &= \frac{1}{2\pi} (1 - g_x u_x - g_y u_y - g_z u_z) \exp\left(-\frac{1}{2}g^2\right) d^3g \\ &= \frac{1}{2\pi} (1 - u_x g \cos \vartheta - u_y g \sin \vartheta \cos \varphi - u_z g \sin \vartheta \sin \varphi) \\ &\quad \times \exp\left(-\frac{1}{2}g^2\right) g^2 \sin \vartheta dg d\vartheta d\varphi \end{aligned} \quad (18)$$

Now we can formulate the equations of motion for the different test particles. We insert the expressions (15) and (18) into Eq. (14) and integrate over the appropriate regions of the relative velocities. We obtain (in reduced units) for a TP with both faces specular reflecting

$$\left. \frac{du_x}{dt} \right|_{\text{specular}} = -\frac{8m}{M+m} u_x \quad (19)$$

The corresponding expressions for a double-side diffuse TP and an asymmetric TP are

$$\left. \frac{du_x}{dt} \right|_{\text{diffuse}} = -\frac{68m}{9(M+m)} u_x \quad (20)$$

$$\left. \frac{du_x}{dt} \right|_{\text{asym}} = -\frac{70m}{9(M+m)} u_x \quad (21)$$

The comparison with (12) yields the corresponding friction coefficients  $\gamma$ . We rewrite the friction coefficients in nonreduced units<sup>(13, 15)</sup>:

$$\begin{aligned} \gamma_{\text{specular}} &= 8nA \frac{m}{M+m} \sqrt{\frac{kT}{2\pi m}} = 2nA \frac{m}{M+m} \langle v \rangle \\ \gamma_{\text{diffuse}} &= \frac{68}{9} nA \frac{m}{M+m} \sqrt{\frac{kT}{2\pi m}} = \frac{17}{9} nA \frac{m}{M+m} \langle v \rangle \end{aligned}$$

The ratio of the friction coefficients of specular and diffuse reflecting particles, respectively, is

$$\frac{\gamma_{\text{diffuse}}}{\gamma_{\text{specular}}} = \frac{17}{18} \quad (22)$$

The friction coefficient of an asymmetric particle is

$$\gamma_{\text{asym}} = \frac{1}{2}(\gamma_{\text{specular}} + \gamma_{\text{diffuse}})$$

In a similar way and without any approximations, one can derive the friction coefficients for the tangential motion of an asymmetric test particle. Obviously, the collisions on the specular side of the TP yield no contribution to the friction force in the tangential direction. Further, due to the uniform distribution of the azimuth reflection angle  $\varphi'$ , the reflected GP on the diffuse side of the TP do not contribute to the damping of the tangential TP velocity. The only contribution arises from the incident particles on the diffuse side. Assuming that the right-hand side of the TP is diffusely reflecting, the equation corresponding to (14, 15) for the tangential TP velocity  $u_x$  reads

$$\frac{du_x}{dt} = -\frac{m}{M+m} \int \int_{g_x < 0} g_x g_x f(\mathbf{g}, \mathbf{u}) d^3g \quad (23)$$

We perform the integration and get

$$\frac{du_y}{dt} = -\frac{m}{M+m} J_r(u_x) u_y \quad (24)$$

$J_r(u_x) = 1/\tau_r(u_x)$  is the incident flux of gas particles to the right-hand side of the TP. For  $u_x=0$ ,  $J_r(0)=1$ , equation (5) holds, and the ratio of the normal to the tangential friction coefficient of an asymmetric test particle is

$$\frac{\gamma_{\text{normal}}}{\gamma_{\text{tangential}}}\bigg|_{\text{asym}}^{(u_x=0)} = \frac{70}{9} \approx 7.8 \quad (25)$$

If the normal velocities  $u_x$  of a TP ensemble are equilibrium distributed, the incident flux of GP to one TP side is  $\sqrt{2}$  (5) and the ratio of the normal to tangential friction coefficients is

$$\frac{\gamma_{\text{normal}}}{\gamma_{\text{tangential}}}\bigg|_{\text{asym}}^{(\text{equilib})} = \frac{70}{9\sqrt{2}} \approx 5.5 \quad (26)$$

In both cases, there is a considerable difference in the friction coefficients and hence in the relaxation times of the normal and tangential degrees of freedom of the asymmetric test particles. This fact becomes important in the future discussion of the relaxation behavior of asymmetric test particles.

Including terms of second order in  $\mathbf{u}$  in the expansion of the distribution function (17) gives for the normal direction "friction force" of an asymmetric TP

$$f(\mathbf{g}, \mathbf{u})^{(2\text{nd order})} = \frac{1}{4\pi} [(g_x^2 - 1) u_x^2 + (g_y^2 - 1) u_y^2 + (g_z^2 - 1) u_z^2 + 2g_x g_y u_x u_y + 2g_x g_z u_x u_z + 2g_y g_z u_y u_z] \exp(-g^2/2)$$

These terms yield the additional contribution

$$\frac{du_x}{dt}\bigg|_{\text{asym}}^{2\text{nd order}} = \frac{m\sqrt{2\pi}}{8(M+m)} \left( u_x^2 - \frac{u_y^2 + u_z^2}{2} \right) \quad (27)$$

to the systematic friction force of the *asymmetric* test particle. For symmetric test particles (both sides specular or both sides diffuse reflecting), the respective second-order terms (27) are identically zero. Now we are able to discuss several special cases of the behavior of an ensemble of asymmetric test particles on the basis of (21) and (27):

1. The equipartition law  $\langle u_x^2 \rangle = \langle u_y^2 \rangle = \langle u_z^2 \rangle$  holds in thermodynamic equilibrium, and the systematic acceleration resulting from (27) vanishes. Additionally,  $\langle u_x \rangle = 0$  holds in equilibrium, and an ensemble of test particles in equilibrium receives no directed acceleration, as expected from the second law of thermodynamics.
2. If the degrees of freedom of the ensemble of asymmetric test particles are not in equilibrium, a resulting *directed* acceleration of the TP follows from (27). The direction of the acceleration depends on the TP velocities of the tangential and normal degrees of freedom, respectively.

## 4.2. Numerical Results

**4.2.1. Equilibrium Properties.** As a check for the numerical method used, we first consider the equilibrium properties of our test particles and compare them with the theoretical predictions. The test quantities are the mean and the mean square TP velocities calculated for a single particle from the time average over  $10^8$  collisions with the gas particles.

The results of the numerical simulation for different test particles are collected in Table I. Here the velocities are shown in units of  $\sqrt{kT/M}$ , differing from the convention mentioned above. In these units the first two moments of the equilibrium velocity distribution (Maxwell distribution) are

$$\langle u_i \rangle = 0, \quad \langle u_i^2 \rangle = 1, \quad i = x, y, z$$

The corresponding values from our simulation (Table I) are in very good agreement with the theoretical predictions; the deviations are within the statistical uncertainties. The numerical method is found to reproduce these equilibrium properties of the test particles correctly.

**4.2.2. Friction Coefficients.** To calculate the friction coefficients, for each kind of TP an ensemble of  $10^8$  test particles with masses  $M/m = 100$  and with fixed initial velocity

$$u_x(t=0) = \sqrt{\langle u_x^2 \rangle}$$

was followed over a time interval  $t = 0 \dots 20\tau_0$  [see Eq. (6)] and the development of the mean velocity of the ensemble in time was determined. (Remember that  $\tau_0$  is the mean time between two impacts on a TP at rest.) With (13) the slope of the logarithmic plot of  $\ln(u/u_0)$  vs.  $t$  yields the friction coefficient of the TP. Figure 2 shows the logarithmic plot of the

**Table I. The First Two Moments of the Velocity Distribution Function of Different Test Particles from a Time Average of a Single Particle over  $10^8$  Collisions<sup>a</sup>**

| $M/m$ | $\langle u_x \rangle$ | $\langle u_x^2 \rangle$ | $\langle u_y \rangle$ | $\langle u_y^2 \rangle$ | $\langle u_z \rangle$ | $\langle u_z^2 \rangle$ | TT  |
|-------|-----------------------|-------------------------|-----------------------|-------------------------|-----------------------|-------------------------|-----|
| 1     | 0.00002               | 0.9998                  | —                     | —                       | —                     | —                       | s/s |
| 10    | 0.00003               | 0.99998                 | —                     | —                       | —                     | —                       | s/s |
| 100   | -0.0007               | 0.9994                  | —                     | —                       | —                     | —                       | s/s |
| 1     | 0.00003               | 1.0001                  | -0.0001               | 0.99994                 | 0.00007               | 1.0002                  | d/d |
| 10    | -0.0001               | 0.9996                  | -0.0002               | 0.999                   | -0.0001               | 1.0007                  | d/d |
| 100   | 0.0002                | 0.9996                  | -0.0004               | 1.001                   | -0.0009               | 0.9995                  | d/d |
| 1     | 0.00003               | 1.00008                 | -0.0001               | 1.00001                 | 0.00002               | 1.00008                 | s/d |
| 10    | 0.0001                | 0.99994                 | -0.0001               | 1.0007                  | -0.0003               | 0.999                   | s/d |
| 100   | -0.001                | 1.0008                  | 0.001                 | 1.00009                 | -0.0006               | 0.999                   | s/d |

<sup>a</sup>The first column shows the mass ratio of test to gas particles, the last column gives the reflection properties of the left- and right-hand sides of the TP, respectively: s = specular, d = diffuse.

mean TP velocities together with the corresponding linear fit curves for a double-side specular and a double-side diffuse reflecting test particle. The slopes of the linear regression lines are

$$\gamma_{\text{diffuse}}^{\text{sim}} = 0.07507, \quad \gamma_{\text{specular}}^{\text{sim}} = 0.07955$$

Both values of the friction coefficient are in excellent agreement with the theoretical results (20) and (19), respectively. The deviations are less than 0.5%, and the ratio of the friction coefficients of 17/18 is confirmed by the simulation.

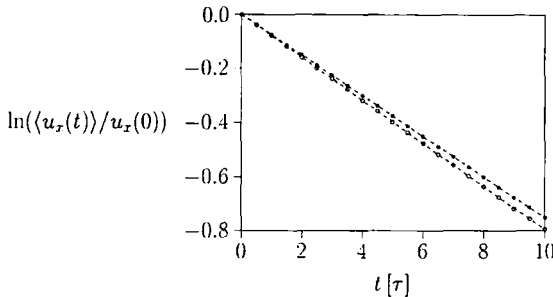


Fig. 2. Logarithmic plot of the mean velocity of an ensemble of  $10^8$  test particles with mass  $M/m = 100$  and a fixed initial velocity: both sides diffuse reflecting (filled circles), both sides specular reflecting (empty circles).

**4.2.3. Directed Acceleration of Asymmetric Test Particles.**

The effect (27) of directed acceleration of a TP ensemble in nonequilibrium is of second order in  $\mathbf{u}$  and decays rapidly with growing mass ratio  $M/m$ . To extract the effect from the noisy background within a reasonable computer time, we choose test particles with masses  $M/m = 1$ . In this case a quantitative comparison with (27) is actually not possible, but the effect suggested by the analytical result for massive test particles should remain even for lower mass ratios  $M/m$ . Thus the existence of a directed acceleration can be shown at least qualitatively.

Figure 3 shows the development in time of the mean velocity of three ensembles of  $10^8$  asymmetric test particles (left-hand side specular reflecting, right-hand side diffuse reflecting) with different initial velocity distributions. The ensemble starting from thermodynamic equilibrium (i.e., initial velocities in all degrees of freedom are Maxwell distributed) shows no directed acceleration. Thus the second law of thermodynamics, forbidding the existence of a *perpetuum mobile* of the second kind, is not violated.

However, the members of an ensemble of asymmetric test particles starting with a nonequilibrium velocity distribution are accelerated on average in a preferred direction as long as thermodynamic equilibrium is not established. The sign of the directed acceleration is given from (27) by

$$2\langle u_x^2 \rangle - (\langle u_y^2 \rangle + \langle u_z^2 \rangle)$$

The angles indicate the average over the entire ensemble.

Even ensembles of TP with initial equilibrium velocity distributions but at different temperature than the gas medium are accelerated in a preferred direction while relaxing to the temperature of their environment. The initial isotropy of the TP velocity distribution is temporarily destroyed

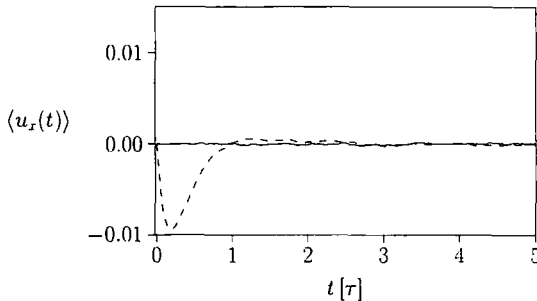


Fig. 3. Mean velocity (in units  $\sqrt{kT/m}$ ) of an ensemble of  $10^8$  test particles with masses  $M/m = 1$  and different initial velocity distributions: (—) all degrees of freedom Maxwell distributed, (···),  $u(0) = 0$ , (- - -),  $u_x(0) = 0$ , tangential degrees of freedom Maxwell distributed.

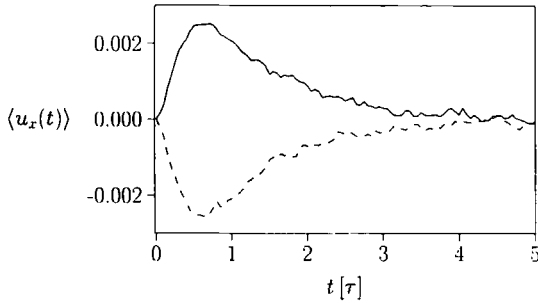


Fig. 4. Mean velocity (in units  $\sqrt{kT/m}$ ) of an ensemble of  $10^8$  test particles with masses  $M/m=1$ . At the starting point, the test particles have an equilibrium velocity distribution corresponding to temperature  $T_0$ , which is different from the temperature  $T_g$  of the gas particles: (—)  $T_0=0.8T_g$ , (---)  $T_0=1.2T_g$ .

by the much faster relaxation of the normal velocity components to equilibrium. The isotropy is restored later after the relaxation of the tangential degrees of freedom of the TP. Thus, if we put (within the framework of our simple model) an ensemble of asymmetric test particles into a gas medium at another temperature, the particles will be shifted on average in one direction as long as a difference in temperature remains. The directed motion of the TP vanishes as the ensemble of TP reaches the temperature of the environment and equilibrium is established (Fig. 4).

For an intuitive explanation of the phenomena shown in Figs. 3 and 4, we consider an asymmetric TP in the special case  $u_x=0$  and  $u_y \neq 0$  in more detail. As in the numerical simulations, the left-hand side of the TP is specular reflecting and the right-hand side is diffuse reflecting.

Now the change of the TP velocity due to the incidence of a GP is (15)

$$\Delta u_x^{(in)} = \frac{m}{M+m} g_x = \frac{m}{M+m} v_x = \frac{m}{M+m} v \cos \theta \quad (u_x=0) \quad (28)$$

For the isotropic velocity distribution of the gas,  $\langle \cos \theta \rangle = 2/3$  holds. The flux of incident GP and the amount of  $\Delta u_x^{(in)}$  are the same on both sides of the TP; thus on the average the incoming GP do not yield an effective acceleration of the TP in the  $x$  direction.

Obviously, the outgoing GP on the specular reflecting side yield the same contribution (28) to  $\Delta u_x$ . On the diffuse reflecting side, in contrast, we have to take into account the full amount of the relative velocity  $g$

$$\Delta u_x^{(out)} = \frac{m}{M+m} g \cos \vartheta' \quad (29)$$

$\cos \vartheta'$  is again isotropically distributed exactly like  $\cos \theta$  in (28). Remark the different meanings of  $\theta$  ( $v_x = v \cos \theta$  in the laboratory system) and  $\vartheta$  ( $g_x = g \cos \vartheta$  in the TP-fixed coordinate system).

Due to the isotropy of the velocity distribution of the GP, the TP is hit with the same probability by a GP having the same velocity component along the  $y$  axis and against the  $y$  axis of the laboratory system, respectively (see Fig. 5). If the test particle is moving with a tangential velocity  $\mathbf{u} = u\mathbf{e}_y$ , the effective relative velocity of the incident particles reads (see Fig. 5)

$$g_{\text{eff}} = \frac{1}{2} [ |\mathbf{v}_1 - \mathbf{u}| + |\mathbf{v}_2 - \mathbf{u}| ] = \frac{1}{2} [ |\mathbf{v}_1 - \mathbf{u}| + |\mathbf{v}_1 + \mathbf{u}| ] \tag{30}$$

The last equality is obvious from symmetry considerations.

All terms in (30) are positive. We square the equation and get

$$g_{\text{eff}}^2 = \frac{1}{4} [ (\mathbf{v}_1 - \mathbf{u})^2 + (\mathbf{v}_1 + \mathbf{u})^2 + 2 |\mathbf{v}_1 - \mathbf{u}| \cdot |\mathbf{v}_1 + \mathbf{u}| ]$$

With the estimation

$$|\mathbf{v}_1 - \mathbf{u}| \cdot |\mathbf{v}_1 + \mathbf{u}| \geq |(\mathbf{v}_1 - \mathbf{u}) \cdot (\mathbf{v}_1 + \mathbf{u})| = |v^2 - u^2|$$

and further  $|v^2 - u^2| \geq v^2 - u^2$  we find

$$g_{\text{eff}}^2 \geq v^2 \tag{31}$$

i.e., the effective amount of the relative velocity is increased due to the tangential velocity of the TP.

In the case of specular reflection, the tangential TP velocity has no influence in (28). On the other hand, as mentioned above,  $\cos \theta$  and  $\cos \vartheta'$  follow the same isotropic distribution function. Thus in the special case considered here ( $u_x = 0, u_y \neq 0$ ), the diffuse side yields a larger contribution to the effective acceleration than the specular reflecting one.

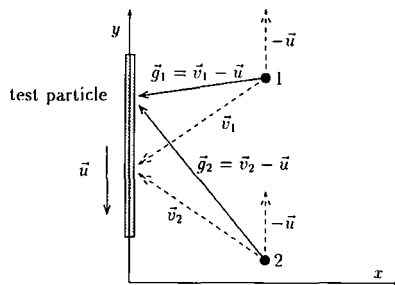


Fig. 5. Test particle and pair of incident gas particles in the TP-fixed coordinate system. The system is moving relative to the laboratory system with the TP velocity  $\mathbf{u} = u\mathbf{e}_y$ , in the  $y$  direction.



One gets an alternative picture by using the total amount of the relative velocity  $g$  and the corresponding angles  $\mathcal{S}' = \mathcal{S}$  also for the description of the specular reflecting side. Now  $g' = g$  holds on both sides, but in the considered case of the anisotropic TP velocities ( $u_x = 0$ ,  $u_y \neq 0$ ),  $\langle \cos \mathcal{S}' \rangle$  is smaller on the specular side than on the diffuse side. (A detailed and more general discussion of the incident angle distribution functions for arbitrary test particles and the corresponding acceleration phenomena is given in the Appendix.)

Thus the resulting asymmetric motion of the TP is caused by the different influence of  $\mathbf{g}$  in the specular and diffuse elastic cases, respectively. The necessary condition for the different contributions of  $\mathbf{g}$  is an anisotropic TP velocity distribution.

In fact, at the very first moment these effects are lacking for isotropic initial velocity distributions of the TP, e.g.,  $\mathbf{p}(\mathbf{u}(0)) = \delta(\mathbf{u})$  (see Figs. 3 and 4). However, as mentioned above, the initial isotropy will be temporarily destroyed until complete equilibrium is reached.

A similar effect was already found for asymmetric particles with one specular reflecting face and one absolutely inelastic face (total accommodation).<sup>(14, 17)</sup>

## 5. SUMMARY

With the simple model of a planar test particle in a rarefied classical gas and the simulation technique presented here, the detailed examination of relaxation to thermal equilibrium of test particles from any initial state is possible. The analytical expressions for the friction coefficients of diffuse and specular reflecting particles with large masses are confirmed by the numerical results. Moreover, the effect of directed acceleration has been shown for asymmetric particles (one side specular reflecting, the other side diffuse-elastic reflecting) in nonequilibrium with the medium. The asymmetric test particles are able to extract directed motion from the white noise of the thermal bath of gas particles as long as they are not completely (i.e., in all degrees of freedom) relaxed to thermodynamic equilibrium. Beside the different systems already discussed in the literature,<sup>(12)</sup> this is another possibility to gain directed transport via spatial asymmetry and a nonequilibrium state from white thermal noise without any external forces or gradients.

## APPENDIX

With a mass ratio  $M/m = 1$  between the TP and the GP, the assumptions made in the derivation of (27) are not valid. For an obvious explanation

of the effects shown in Figs. 3 and 4, the following considerations are helpful: In all cases examined by our numerical simulation, the initial velocity distribution of the ensemble of TP is symmetric around 0 in the  $x$  direction. Consequently, the flux of incident particles and the mean amount of their relative velocities are the same on both sides of the TP. Under these conditions, the sign of the mean acceleration of the TP ensemble follows from the sum of the velocity changes due to impacts on both sides of the asymmetric test particle (15):

$$\dot{u}_x \sim \Delta u_x^{(l)} + \Delta u_x^{(r)} \sim \langle \cos \vartheta \rangle - \frac{2}{3} \quad (\text{A1})$$

$\langle \cos \vartheta \rangle$  is the mean cosine of the reflection angles on the specular side of the TP. The value  $2/3$  follows from (16) for the reflection angles on the diffuse side and is independent of the state of motion of the TP.

If we know the distribution function of the incident angles  $\vartheta$  of the GP (which is equal to the distribution function of the specular reflected GP), we can determine the sign of the mean acceleration of the TP ensemble.

To derive expressions for  $\langle \cos \vartheta \rangle$ , we again consider the left-hand side of the test particle. The velocity distribution function of the incident gas particles is

$$\rho(\mathbf{v}) d^3v \sim (v_x - u_x) \exp(-\frac{1}{2}\mathbf{v}^2) d^3v \quad (\text{A2})$$

By multiplying (A2) with the velocity distribution  $p(\mathbf{u})$  of the TP, we get the probability density for a collision between a test particle with velocity  $\mathbf{u}$  and a gas particle with velocity  $\mathbf{v}$ .

For the distribution function of the TP velocities, we make the following ansatz:

$$p(\mathbf{u}) = \frac{\alpha_t}{2\pi} \sqrt{\frac{\alpha_n}{2\pi}} \exp\left(-\frac{\alpha_n}{2} u_x^2\right) \exp\left[-\frac{\alpha_t}{2}(u_y^2 + u_z^2)\right] \quad (\text{A3})$$

The parameters  $\alpha_n$  and  $\alpha_t$  determine the temperatures or the degrees of relaxation to equilibrium of the normal ( $x$ ) and tangential ( $y, z$ ) degrees of freedom of the TP, respectively.

$\alpha_i = 1$  corresponds to the equilibrium Maxwell distribution of the respective velocity component. With  $\alpha_i \rightarrow \infty$ , the distribution function of the corresponding velocity component tends to the delta function  $\delta(u_i)$ .

Now we are able to construct the velocity distribution functions  $p(\mathbf{u})$  of the different test particle ensembles investigated in Figs. 3 and 4. As an example, we consider the ensemble of TP with the initial condition

$\mathbf{u}(0) = \mathbf{0}$ . In this simplest case, the joint probability density of the TP and GP velocities reads

$$\rho(\mathbf{v}, \mathbf{u}) d^3v d^3u \sim (v_x - u_x) \exp(-\frac{1}{2}v^2) \delta(\mathbf{u}) d^3v d^3u \quad (\text{A4})$$

We transform (A4) to the center-of-mass system by

$$\mathbf{v} = \mathbf{s} + \frac{1}{2}\mathbf{g} \quad \text{and} \quad \mathbf{u} = \mathbf{s} - \frac{1}{2}\mathbf{g} \quad (\text{A5})$$

$\mathbf{g} = \mathbf{v} - \mathbf{u}$  is the relative velocity between TP and GP, and  $\mathbf{s}$  is the center-of-mass velocity of TP and GP. In the transformation rules (A5) the mass ratio  $M/m = 1$  is used.

The probability density (A4) transformed to the center-of-mass system reads

$$\rho(\mathbf{s}, \mathbf{g}) d^3s d^3g \sim g_x \exp[-\frac{1}{2}(\mathbf{s} + \frac{1}{2}\mathbf{g})^2] \delta(\mathbf{s} - \frac{1}{2}\mathbf{g}) d^3s d^3g \quad (\text{A6})$$

The integration over the center-of-mass velocities is trivial and yields the probability density of the relative velocity

$$\rho(\mathbf{g}) d^3g \sim g_x \exp(-\frac{1}{2}g^2) \quad (\text{A7})$$

Now we transform the distribution function (38) to spherical polar coordinates and integrate over the azimuth angle  $\varphi$  from 0 to  $2\pi$  and over the amount of the relative velocity  $g$  from 0 to  $\infty$ . With the appropriate normalization, we finally arrive at the distribution function of the incident angles  $\vartheta$

$$2 \cos \vartheta \sin \vartheta d\vartheta \quad (\text{A8})$$

In the same way we get the distribution functions of the incident angles for ensembles of TP in different initial states. In the general case of arbitrary values of the parameters  $\alpha_n$  and  $\alpha_l$ , the incident angle distribution function reads

$$\frac{2\alpha_n\alpha_l \cos \vartheta}{(\alpha_n + 1)(\alpha_l + 1) \{ [\alpha_n/(\alpha_n + 1)] \cos^2 \vartheta + [\alpha_l/(\alpha_l + 1)] \sin^2 \vartheta \}^2} \sin \vartheta d\vartheta \quad (\text{A9})$$

For the cases of interest (see Figs. 3 and 4), the values of  $\langle \cos \vartheta \rangle$  due to the respective distribution functions (A9) can be calculated:

$$\mathbf{u} \text{ eq} \Rightarrow \langle \cos \vartheta \rangle = \frac{2}{3} \approx 0.67 \quad (\text{A10})$$

$$\mathbf{u} = \mathbf{0} \Rightarrow \langle \cos \vartheta \rangle = \frac{2}{3} \approx 0.67 \quad (\text{A11})$$

$$u_x \text{ eq, } u_y = u_z = 0 \Rightarrow \langle \cos \vartheta \rangle \approx 0.75 \quad (\text{A12})$$

$$u_x = 0, \quad u_{y,z} \text{ eq} \Rightarrow \langle \cos \vartheta \rangle = \frac{1}{2}\pi - 1 \approx 0.57 \quad (\text{A13})$$

The abbreviation eq stands for equilibrium distribution, i.e., the respective initial velocity components are Maxwell distributed and in equilibrium with the gas medium.

On the basis of (32) and (A11)–(A12) the results of the numerical simulation of asymmetric test particles shown in Figs. 3 and 4 find a simple qualitative explanation:

The mean acceleration of an ensemble of TP in equilibrium (A10) is zero.

For a TP ensemble initially at rest (A11), the initial mean acceleration is zero, too. However, due to the much faster relaxation to equilibrium of the normal degree of freedom [Eqs. (25) and (26)], the ensemble of TP first approaches the state (A12). In that state, the mean acceleration (32) is  $\dot{u}_x > 0$ . After the relaxation of the tangential degrees of freedom, the mean acceleration of the TP ensemble vanishes.

From the initial state (A13), the TP ensemble starts with a mean acceleration  $\dot{u}_x < 0$ . The full equilibrium state is reached earlier than in the preceding case due to the faster relaxation of the normal degree of freedom.

In a similar way, we can discuss the behavior of the ensembles of asymmetric test particles shown in Fig. 4. At the starting point,  $\alpha_n = \alpha_t = \alpha$  holds. [Remember that  $\alpha > (<) 1$  corresponds to an ensemble of TP at lower (higher) temperature than the gas medium.] After a relatively short time, the normal degree of freedom of the test particles is relaxed to equilibrium (i.e.,  $\alpha_n = 1$ ), while for the tangential velocities  $\alpha_t \neq 1$  still holds. In this state, (A9) and (32) yield

$$\alpha_t > 1 \text{ (i.e., } T_0 < T_m) \Rightarrow \langle \cos \theta \rangle > \frac{2}{3} \Rightarrow \dot{u}_x > 0 \quad (\text{A14})$$

$$\alpha_t < 1 \text{ (i.e., } T_0 > T_m) \Rightarrow \langle \cos \theta \rangle < \frac{2}{3} \Rightarrow \dot{u}_x < 0 \quad (\text{A15})$$

which is exactly what we see in Fig. 4.

## REFERENCES

1. A. Einstein, *Ann. Phys.* (Leipzig) 17:549 (1905).
2. D. L. Ermak and J. A. McCammon, *J. Chem. Phys.* 69(4):1352 (1978).
3. G. Ciccotti and J.-P. Ryckaert, *J. Mol. Phys.* 40(1):141 (1980).

4. J. F. Fernández and J. Marro, *J. Stat. Phys.* **71**(1/2):225 (1993).
5. W. Schaertl and H. Sillescu, *J. Stat. Phys.* **74**(3/4):687 (1994).
6. S. Chandrasekhar, *Rev. Mod. Phys.* **15**:1 (1943).
7. J. R. Dorfman and E. G. D. Cohen, *Phys. Rev. A* **6**(2):776 (1972).
8. D. Levesque and W. T. Ashurst, *Phys. Rev. Lett.* **33**(5):277 (1974).
9. J. J. Erpenbeck and W. W. Wood, *Phys. Rev. A* **26**(3):1648 (1982).
10. J. Marro and J. Masoliver, *J. Phys. C* **18**:4691 (1985).
11. H. M. Schaink and C. Hoheisel, *Phys. Rev. A* **45**(12):8559 (1992).
12. S. Leibler, *Nature* **370**:412 (1994).
13. K. Handrick, *Sov. Phys. JETP* **69**(3):513 (1989).
14. U. Heiber, Ph.D. thesis, Chapter 2, University of Ilmenau, Germany (1995).
15. R. S. Modak, *Am. J. Phys.* **52**(1):43 (1984).
16. L. M. Raff, J. Lorenzen, and B. C. McCoy, *J. Chem. Phys.* **46**(11):4265 (1967).
17. K. Handrick and U. Heiber, To be published.